THE MIGRATION OF RADIOACTIVE BERYLLIUM
IN THE ISX-B TOKAMAK

A. C. England
D. L. Hillis
P. H. Edmonds

CONTENTS

ABSTRACT

One of 12 beryllium tiles on a top rail limiter in the Impurity Study Experiment (ISX-B) tokamak was intentionally made radioactive. The migration of the radioactivity due to melting, ablation, and general excoriation of the radioactive tile was studied. Several hundred milligrams of material from the radioactive tile were spread to the other tiles over the course of the experiment, which consisted of more than 3000 tokamak shots. A small amount of activity was found on the bottom of the tokamak vacuum vessel. The distribution of activity on the other limiter tiles showed a marked radially inward directivity, although all of the tiles received some activity. The possibility that some of the activity was the result of photo- and electro-excitation by runaway electrons cannot be ruled out but probably cannot account for the bulk of the effect.

1. INTRODUCTION

The beryllium limiter experiment was performed on the Impurity Study Experiment (ISX-B) at Oak Ridge National Laboratory (ORNL) to study the suitability of beryllium as a limiter material in a large tokamak such as the Joint European Torus (JET). The beryllium limiter has been described elsewhere [1,2], and the main results are the subject of other studies. The limiter was a rail type, used as the upper limiter and oriented along a major radius. It was composed of 12 tiles bolted to a stainless steel back plate for thermal and electrical contact. To study the migration of beryllium from tile to tile on the limiter, one tile was made radioactive. Figure 1 shows the limiter assembly from the side with the radioactive tile pulled out and rotated to show its shape. The tips of the tiles faced the plasma, and their position determined the minor radius of the plasma. The radioactive tile
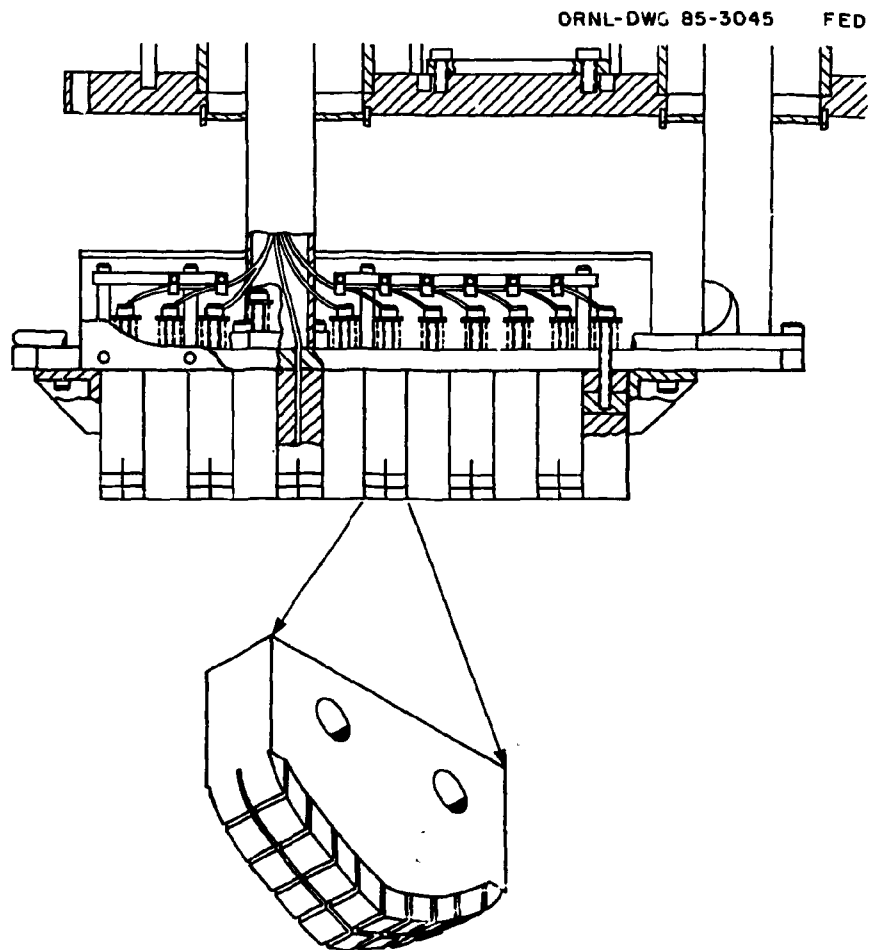
ORNL-DWG 85-3045   FED

FIGURE 1. The Be limiter assembly. The radioactive tile is shown pulled out and rotated to illustrate the tesselated construction. The tesselations were produced by cutting slots ~1 cm apart in the front surface. The large major radius side is to the right.

was one of six tesselated tiles mounted alternately with six plain tiles. The tesselations were produced by cutting slots in the surface with a spacing of ~1 cm.

Natural beryllium is 100% ^{9}Be. The only convenient long-lived radioisotope of beryllium is ^{7}Be, which has a half-life of 53.37 days. The isotope ^{7}Be decays by electron capture and produces a 478-keV gamma ray that is easily distinguished. The only other radioisotope of beryllium is ^{10}Be, which has a half-life of 2.5 × 10^6 years and is subject to beta decay with no convenient identifiable gamma ray. Producing some ^{7}Be activity in one tile would allow the beryllium to remain beryllium and to act chemically and physically like the remaining material.

The isotope ^{7}Be can be obtained in volume by irradiating beryllium in a flux of high-energy X rays, which can be produced by means of an electron linear accelerator. The reaction needed is ^{9}Be(γ,2n)^{7}Be, which has a Q of -20.56. Hence, X rays of energy higher than 20.6 MeV are needed. The Oak Ridge Electron Linear Accelerator (ORELA) was used to produce the desired activity. The metal tiles used in the experiment were made of high-purity beryllium and therefore had no trace impurities that could be activated by other techniques such as neutron irradiation.

Figure 2 is a photograph of the limiter taken near the end of the experiment. The radioactive tile is the sixth tile from the right. During the course of the experiment, the limiter experienced more than 3000 tokamak shots, many of which employed neutral-beam heating at power levels up to ~0.9 MW. Most of the damage observed here occurred during the high-current, high-beam-power shots.
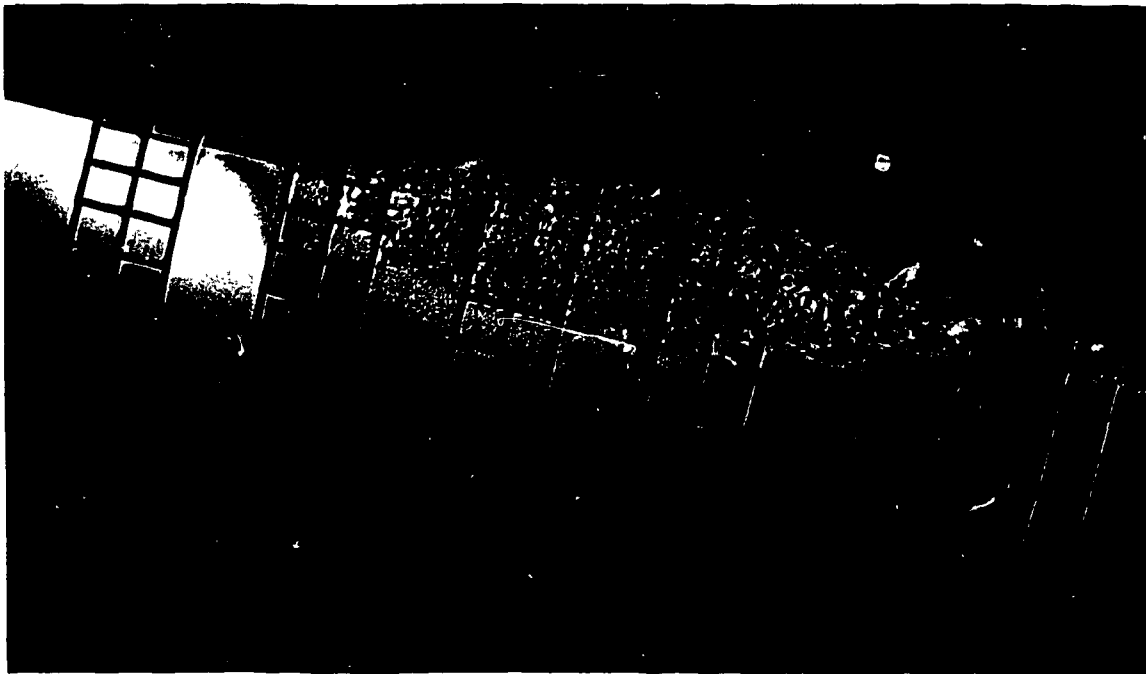
ORNL PHOTO 8536-85

FIGURE 2. Photograph of the Be limiter near the end of the experiment. The radioactive tile is the sixth from the right side.

Previously, an activation experiment using ^{48}V in a titanium plate on the Divertor and Injection Tokamak Experiment (DITE) was used to study erosion of the titanium divertor target by Goodall et al. [3]. Activation has also been used to study sputtering yields by Switkowski et al. [4].

2. VOLUME PRODUCTION OF ^{7}Be

The integral cross section (in units of MeV-mb) for ^{7}Be production was measured by Lokan [5] at 30 MeV and by Foster and Voight [6] at 45 MeV. There are no measurements near 120 MeV, the energy appropriate for ORELA. The total photonuclear cross section for ^{9}Be has been measured up to 140 MeV [7], but that due to (γ,2n) was not specifically determined. The required exposure was determined by trial and error because it was not possible to make a good estimate of it at ORELA based on the available cross section data.

For the irradiation, a beryllium tile was mounted in a graphite holder behind the tantalum target and electron catcher normally used at ORELA. The tip of the limiter tile was set facing the incident X-ray beam. The beryllium tile was exposed for approximately 12-h with an electron energy of ~120 MeV. Small beryllium cubes were mounted behind the beryllium tile and exposed to the flux of X rays coming through the tile. Each cube had been weighed so that the activity per unit mass of the tile could be determined. The seven small cubes were spaced 1.27 cm apart along the 9.52-cm tile length during the irradiation.

3. EXPERIMENTAL SET-UP

The γ-ray detection system consisted of two 7.62- by 7.62-cm (3- by 3-in.) NaI(Tl) crystals on phototubes facing each other at a spacing of 1.3 to 2.5 cm depending on the sample being counted. The two signals were summed and counted. The stainless steel squares from the bottom of ISX-B (described in Sect. 5.1) were inserted into holes in two surrounding 12.7- by 12.7-cm (5- by 5-in.) NaI(Tl) crystals used as anticoincidence shields. The signals from the phototubes were routed as shown in Fig. 3.

For counting the limiter tiles that would not fit into the anticoincidence shield, the two 7.62- by 7.62-cm crystals were set facing each other at a separation of 2.54 cm. No anticoincidence was used in these measurements, resulting in a somewhat higher background. In all cases, the counting devices were surrounded by a lead shield to reduce the background.

4. MEASUREMENT TECHNIQUES

The limiter tile was mounted in ISX-B a few days after the ORELA exposure. The total duration of the experiment from limiter installation to removal was ~120 days. The limiter tiles and samples were counted on the fifth and sixth day after removal from ISX-B. During the several months between start and finish, the activity of the irradiated beryllium cubes was followed (1) to determine the detection efficiency of the crystals and (2) to ensure that the activity actually was ^{7}Be with a half-life of ~53 days. The count rates from the NaI crystals could be extrapolated back to the time of the irradiation.
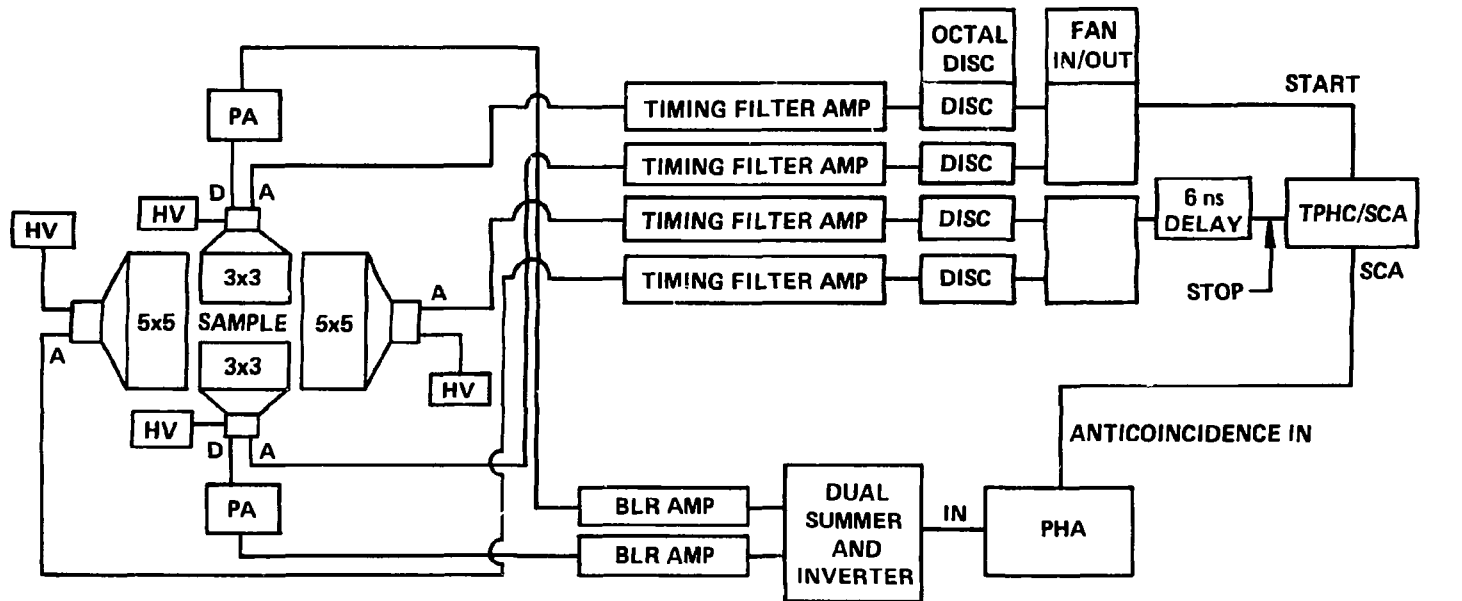
FIGURE 3. Circuit diagram of the counting and anticoincidence arrangement. The anticoincidence 5- by 5-in. crystals surrounded the 3- by 3-in. crystals. During the counting of the large tiles, the smaller crystals were removed from inside the larger crystals and the anticoincidence disabled.

Using the accurately determined activity measured at ORELA, a comparison could be made between the count rate and the activity, which determined the efficiency of the counting arrangement.

The data were also corrected for the γ-ray attenuation of the stainless steel for the samples from the bottom of the vacuum tank. The effect of the position of the activity on the beryllium tile surfaces was checked by mounting a small beryllium cube on the surface of an unused tile and measuring the count rate as a function of position of the cube.

The most active tile of the originally unactivated tiles was the one just adjacent to the activated tile toward the inside of ISX-B. Because of its high activity, simple collimator measurements could be made with a lead collimator. The uniformity of the activity of the irradiated tile was also checked in this way after it was removed from ISX-B.

5. RESULTS

5.1 Stainless Steel Samples

Seven stainless steel samples were placed on the bottom of the ISX-B vacuum tank. Each one was 0.3175 cm × 3.81 cm × 3.81 cm (0.125 × 1.5 × 1.5 in.). Each originally had a small piece of silicon mounted on it that was removed before the counting. Of the seven samples in the vacuum chamber, only three showed any color change (a slight yellow tinge) due to the exposure. On the surface of two of these, small metal droplets, presumably beryllium metal, were deposited. Only one sample, the one that had been placed directly below the limiter, displayed any activity.

A comparison of the measured activity in the sample to one of the calibrated beryllium cubes showed that the amount of mass represented by the activity was between 125 and 250 μg, assuming that the mass came from the tip of the radioactive tile. This is the estimated amount of mass in the small solidified droplets on the surface of the sample. The minimum amount of detectable radioactive material from the tip of the radioactive tile is estimated to be 60 to 120 μg based on counting statistics (one standard deviation).

5.2 Nonirradiated Limiter Tiles

Each of the nonirradiated limiter tiles was counted with the two 7.62- by 7.62-cm NaI crystals facing each other and separated by ~2.5 cm. The anticoincidence arrangement could not be used because the limiter tiles did not fit inside the anticoincidence crystal assembly; hence, the background was somewhat higher. Due to measures taken for safety, the reproducibility of position was not good and was estimated to be ±0.6 cm. The tiles were counted with the tip of the tile on the axis of the two facing crystals.

The activity in the tiles was compared to the activity measured from a previously calibrated beryllium cube mounted on the centerline of the crystals. This position gives the maximum solid angle for γ-ray detection. The activity on the beryllium tiles could therefore be related to an equivalent amount of material on the tip of the irradiated tile, which is the minimum amount of material that could be responsible for the observed count rate. This activity and the equivalent mass of material transferred from the tip of the irradiated tile are given in Table 1 and presented in Fig. 4. For Table 1, the tiles have been numbered in order from the outside (large major radius side) inward. The radioactive tile was tile 6. The geometric center was between tiles 6 and 7.

TABLE 1. ACTIVITY ON Be TILES AND EQUIVALENT MASS OF MATERIAL TRANSFERRED

Tile	Activity (nCi)	Active material deposited (mg)	Mass change (mg)	Type[a]	Comments
1	0.05	1.2	+1.1	P	Outermost
2	0.09	2.0	+2.6	T	
3	0.09	2.1	−9.2	P	
4	0.18	4.3	−89.5	T	
5	0.53	12.3	−323.5	P	
6			−1110.8	T	Activated tile
7	18.0	422	−742.5	P	
8	6.56	154	−896.1	T	
9	2.17	50.9	+146.2	P	
10	≥2.14	≥50.2	+882.6	T	Long projection
11	0.31	7.3	+40.0	P	
12	0.46	10.8	+95.7	T	Innermost

[a]The type refers to tesselated (T) or plain (P).

Measurements were made with calibrated beryllium cubes at other points on the unused tile. For locations about 2.5 cm from the tip, the counting rate was about 85% of the activity on the tip. For locations near the edge of the crystals, the activity was about 50% of the activity on the tip. Simple collimator measurements (described in Sect. 5.3) showed no activity beyond this distance on the limiter surfaces. Hence, we conclude that the values in Table 1 and Figure 4 are not more than a factor of two in error and represent the minimum amount of material transferred from the center of the irradiated tile, provided that no additional activity was generated on the surface by runaways.

The tiles were weighed before and after the experiment. The amount of material lost from or gained by each tile is displayed in column 4 of Table 1. It is clear from the table that the amount of material represented by the activity transferred to the other tiles is less than the mass loss of the activated tile, which lost 1.111 g of mass. The minimum equivalent mass represented by the activity of all the other tiles is 0.716 g. Tiles 3 through 8 suffered a net loss of mass, but presumably tiles 3, 4, 5, 7, and 8 gained some mass from tile 6, as evidenced by the measured activity.

It was not possible to insert tile 10 into the space between the crystals because a protuberance of metal had grown on its surface. Hence, the tile could not be measured in the same geometry. The value given in Table 1 and Fig. 4 is a minimum value and could be higher by a factor of two, depending on the exact location of the activity. The mass gain of tile 10 is the largest single gain of any tile.
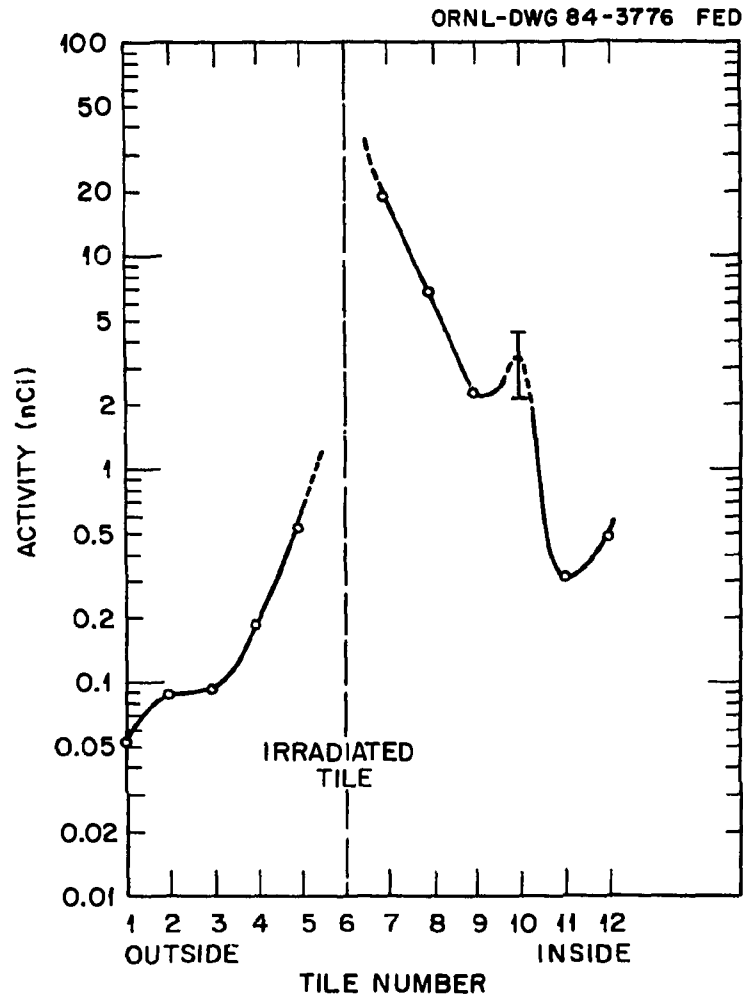
ORNL-DWG 84-3776 FED

FIGURE 4. Activity (nCi) as a function of tile number on the rail limiter. The activity of tile 6 is too high to be represented here. The activity of tile 10 could not be accurately determined due to a projection that had grown on the tile.

As shown in Table 1 and Fig. 4, the material seems to have moved predominantly from the irradiated tile toward the inside of the machine (i.e., toward the smaller major radius side). This is consistent with the observation that the solidified droplets on the surface of the tiles show a general pattern of inward directivity, presumably produced by $j \times B$ forces on the molten material. The unipolar arc tracks visible on the surface of the limiter are always found to move in the retrograde $j \times B$ direction, and the direction of B was held constant for most of the experiment. The direction of $j \times B$ determined from these conditions implies that j was usually out of the upper limiter into the plasma. The activity on the outer tiles could have been moved there by $j \times B$ forces during the short period of time when the magnetic field was reversed. In addition, it is possible that the activity could have been transferred by the splattering of molten material. It is also possible that some of the activity was produced by runaways.

TABLE 1. ACTIVITY ON Be TILES AND EQUIVALENT MASS OF MATERIAL TRANSFERRED

Tile	Activity (nCi)	Active material deposited (mg)	Mass change (mg)	Type[a]	Comments
1	0.05	1.2	+1.1	P	Outermost
2	0.09	2.0	+2.6	T	
3	0.09	2.1	−9.2	P	
4	0.18	4.3	−89.5	T	
5	0.53	12.3	−323.5	P	
6			−1110.8	T	Activated tile
7	18.0	422	−742.5	P	
8	6.56	154	−896.1	T	
9	2.17	50.9	+146.2	P	
10	≥2.14	≥50.2	+8°2.6	T	Long projection
11	0.31	7.3	+40.0	P	
12	0.46	10.8	+95.7	T	Innermost

[a]The type refers to tesselated (T) or plain (P).

Measurements were made with calibrated beryllium cubes at other points on the unused tile. For locations about 2.5 cm from the tip, the counting rate was about 85% of the activity on the tip. For locations near the edge of the crystals, the activity was about 50% of the activity on the tip. Simple collimator measurements (described in Sect. 5.3) showed no activity beyond this distance on the limiter surfaces. Hence, we conclude that the values in Table 1 and Figure 4 are not more than a factor of two in error and represent the minimum amount of material transferred from the center of the irradiated tile, provided that no additional activity was generated on the surface by runaways.

The tiles were weighed before and after the experiment. The amount of material lost from or gained by each tile is displayed in column 4 of Table 1. It is clear from the table that the amount of material represented by the activity transferred to the other tiles is less than the mass loss of the activated tile, which lost 1.111 g of mass. The minimum equivalent mass represented by the activity of all the other tiles is 0.716 g. Tiles 3 through 8 suffered a net loss of mass, but presumably tiles 3, 4, 5, 7, and 8 gained some mass from tile 6, as evidenced by the measured activity.

It was not possible to insert tile 10 into the space between the crystals because a protuberance of metal had grown on its surface. Hence, the tile could not be measured in the same geometry. The value given in Table 1 and Fig. 4 is a minimum value and could be higher by a factor of two, depending on the exact location of the activity. The mass gain of tile 10 is the largest single gain of any tile.
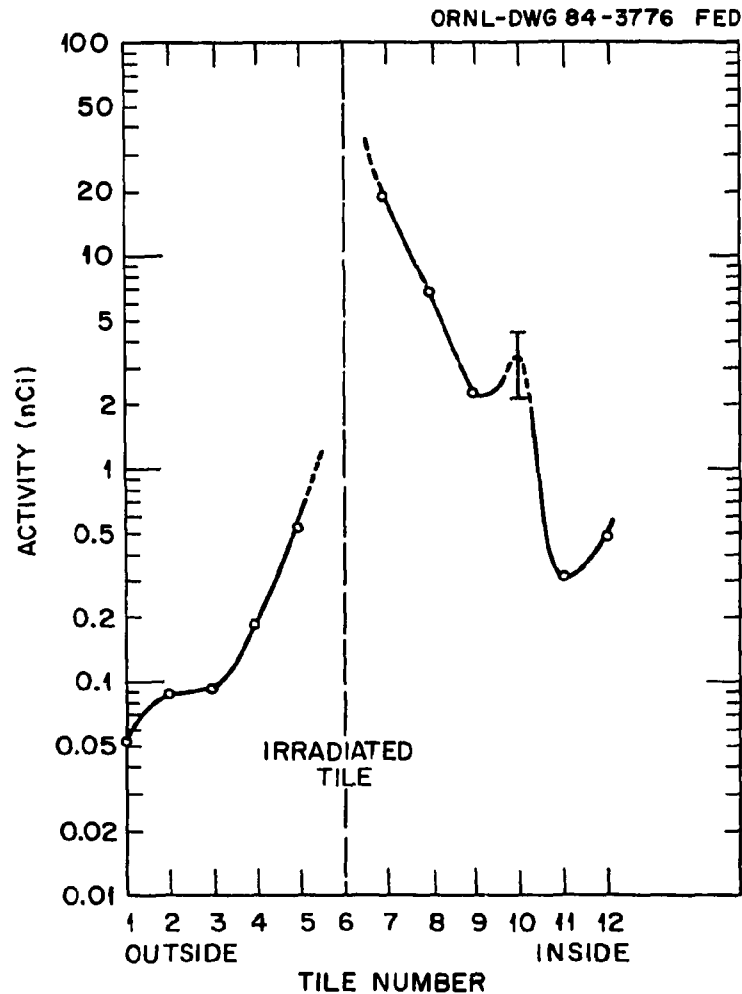
ORNL-DWG 84-3776 FED

FIGURE 4. Activity (nCi) as a function of tile number on the rail limiter. The activity of tile 6 is too high to be represented here. The activity of tile 10 could not be accurately determined due to a projection that had grown on the tile.

As shown in Table 1 and Fig. 4, the material seems to have moved predominantly from the irradiated tile toward the inside of the machine (i.e., toward the smaller major radius side). This is consistent with the observation that the solidified droplets on the surface of the tiles show a general pattern of inward directivity, presumably produced by $j \times B$ forces on the molten material. The unipolar arc tracks visible on the surface of the limiter are always found to move in the retrograde $j \times B$ direction, and the direction of B was held constant for most of the experiment. The direction of $j \times B$ determined from these conditions implies that j was usually out of the upper limiter into the plasma. The activity on the outer tiles could have been moved there by $j \times B$ forces during the short period of time when the magnetic field was reversed. In addition, it is possible that the activity could have been transferred by the splattering of molten material. It is also possible that some of the activity was produced by runaways.

5.3 Collimator Measurements

Measurements of the activity of the irradiated tile were made after its removal from ISX-B. Figure 5 shows the result of a scan across the length of the tile. The resolution is ~1 cm, as determined by the collimator. Superimposed on this graph is the activity from the calibrated beryllium cubes that were mounted behind the tile during the irradiation in ORELA. The activity for the cubes has been normalized to the activity on the tile at the location of cube 6 and is so plotted. It represents an increase of a factor of about 26 over the activity of the cubes measured in the same set-up as the simple collimator measurements of the irradiated tile.

Calculations show that the count rate due to the irradiated limiter tile should be about 20 times higher than for the beryllium cubes due to the larger volume of material visible to the NaI crystal through the collimator. There is an additional factor of about 1.05 due to
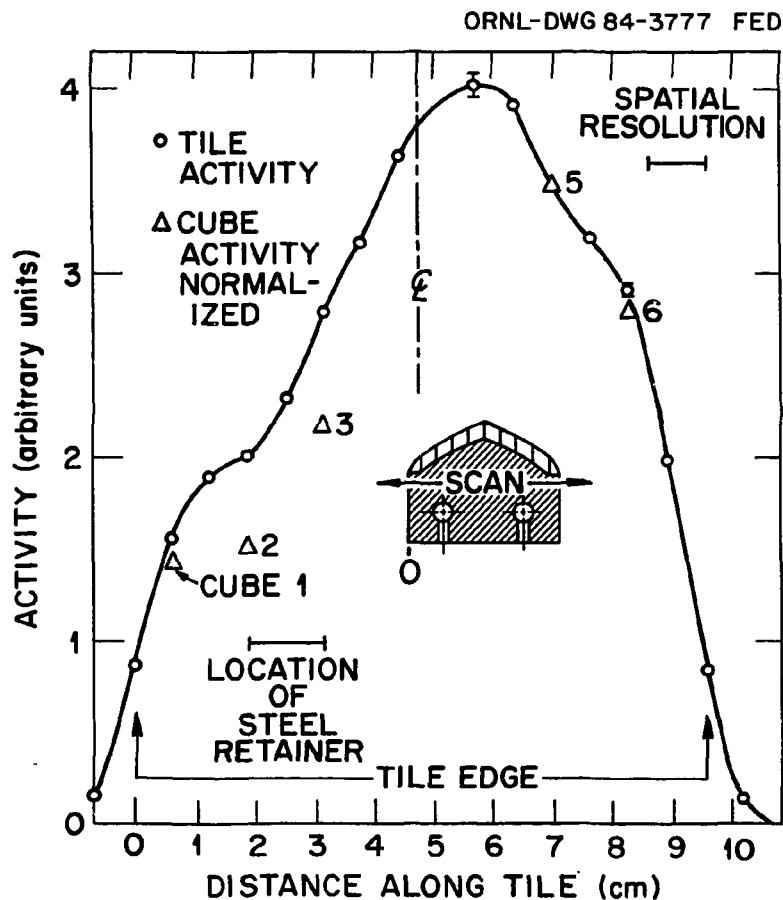
ORNL-DWG 84-3777 FED

FIGURE 5. Collimator scan across the length of the activated tile at the position shown in the insert. Also shown are the activities of the beryllium cubes normalized to the tile activity at the position of cube 6. Note that the peak of the activity does not coincide with the center line of the limiter tile.

the fact that the center of the tile, where the scan was made, was somewhat more active than the back. It is believed that uncertainties in position can account for the additional difference between these measurements. The activity of cubes 2 and 3 is anomalously low. These cubes were directly behind a piece of steel that held the beryllium tile to the support during the irradiation and hence did not receive the same dose as the front of the tile.

It is noted from Fig. 5 that the tip of the irradiated tile does not coincide with the peak of the activity, which is displaced by about 1 cm. This resulted from the original irradiation at ORELA due to a lack of knowledge about the exact location of the electron beam. The strong peaking of the activity was also unexpected and resulted from a lack of knowledge about the X-ray angular distribution from the tantalum target at ORELA. The full width at half-maximum of the activity represents an angular width of ~7° as viewed from the tantalum target.

A vertical collimator scan from the tip of the irradiated tile to the bottom of the tile is shown in Fig. 6. The purpose of this scan was to determine the uniformity of activity. This scan was expected to reveal (1) if the activities of the beryllium cubes were representative
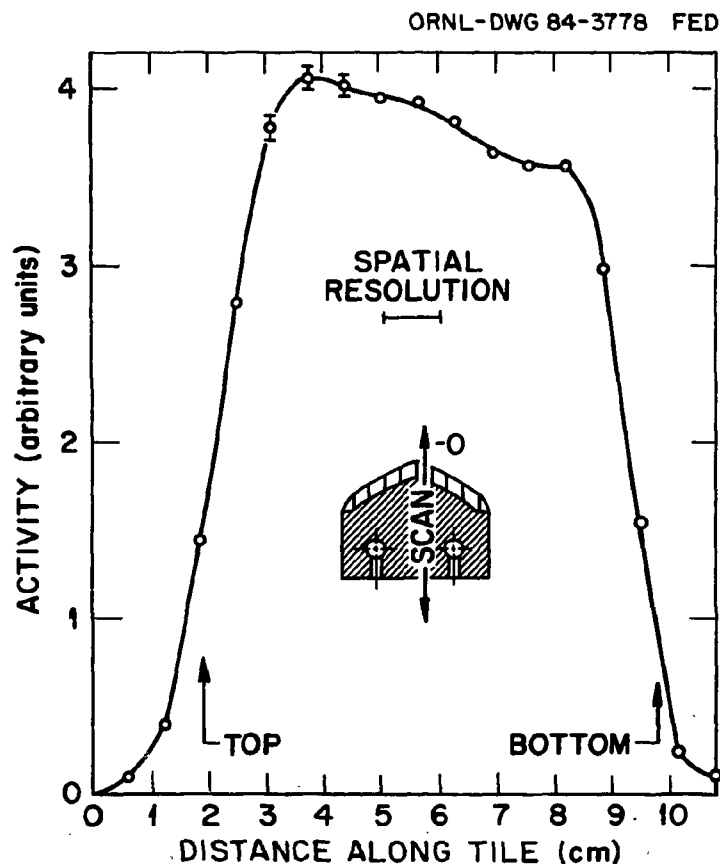
ORNL-DWG 84-3778 FED

FIGURE 6. Collimator scan from top to bottom of the activated tile. The activity at the front appears to be ~10% higher than that at the back.

of that in the front surface of the tile and (2) if additional activity could have been produced on the front surface by runaway electrons.

From the figure it appears that the front has about 10% higher activity than the back. The resolution is again about 1 cm. Due to the poor resolution, it is not possible to determine any very local increase in activity on the surface, so the issue of surface activation by runaways cannot be answered by this technique. The gradual trend of decreasing activity from front to back was expected from the original irradiation.

6. DISCUSSION

An important question can be asked: Can relativistic electrons be contained in ISX-B with energies in excess of the threshold energy for $(\gamma,2n)$ reactions in beryllium? From Knoepfel and Spong [8] the maximum electron energy in ISX-B can be calculated. Relativistic electron orbits are shifted outward as the energy increases. For a uniform plasma current distribution, the outward shift is given by Eq. (4.19) of Ref. 8:

$$d_\gamma = \frac{a_r^2}{2R} \times \frac{I_A}{I} \ ,$$

where a_r is the minor radius of the plasma in ISX-B (26 cm), R is the major radius (93 cm), I_A is the Alfvén current, and I is the plasma current.

The Alfvén current is given by

$$I_A \ (\text{kA}) = 17(\gamma^2 - 1)^{1/2} \ ,$$

where $\gamma = E/mc^2 + 1$ and E is the electron kinetic energy. For the beryllium limiter experiment, the usual plasma current was 100 kA, but there were some shots at 116 kA and several others at currents up to 176 kA. The outer limiter was a TiC-coated graphite mushroom limiter set to allow a plasma minor radius of $a_r = 26$ cm. This defines the maximum minor radius for runaway electrons. The Be top rail limiter was positioned to allow $a_p = 24$ cm, and this defined the bulk plasma minor radius.

For the ISX-B experiment, Table 2 gives the electron energy, γ, I_A, and the outward shift d_γ for 100-kA plasma current shots. It is clear from the table that for electron energies in excess of 21 MeV there is no containment, as the shift exceeds the minor radius defined by the TiC-coated graphite mushroom limiter.

Inclusion of current peaking modifies this value somewhat, as does feedback control, which can center the plasma somewhere other than the geometric center of the chamber. For this experiment, the current was generally centered. From Fig. 12 of Ref. 8, we can find that for a peaked current profile of the form $j(r) = j(0)[1 - (r/a_r)^n]$, somewhat higher energies are permitted. For $n = 3$, 22-MeV electrons may be contained, and for $n = 1$ (very peaked), 23-MeV electrons can be contained. However, no condition can be found that permits the containment of 24- to 30-MeV electrons.

TABLE 2. STATISTICS FOR 100-kA PLASMA CURRENT SHOTS

E_e (MeV)	γ	I_A (kA)	d_γ (cm)
20	40.14	682.2	24.8
21	41.00	698.7	25.39
22	43.05	731.7	26.59
23	45.01	765.0	27.80

The beryllium limiter was the upper limiter near the major radius, and relativistic electron orbits are confined to drift surfaces near the midplane at the outer limiter position, far from the beryllium limiter. The drift surface radii for these very relativistic particles are quite small, typically a few centimeters, and they would not touch the upper limiter.

Reference 8 does not discuss the effect of disruptions. During a disruption, it is possible to accelerate electrons, and the drift surfaces may not be constrained as indicated by the preceding discussion. During the beryllium limiter experiment, there were frequent disruptions. It is possible that relativistic electrons with energies higher than 23 MeV may have struck the upper limiter during these events. On JET, preliminary observations show that during disruptions relativistic electrons strike the inner wall and cause melting and activation [9]. However, there is currently no evidence of activity on the top and outer wall of the vacuum vessel. The energies are high (>23 MeV) based on the Q value of the observed reactions.

A second question to be addressed is whether runaways could produce sufficient bremsstrahlung to produce the measured activation. According to Koch and Motz [10], the total amount of bremsstrahlung energy produced in thick targets is given by

$$P_{tot} = 1 \times 10^{-3} Z(E - k)$$

for electron energies up to 5 MeV, where Z is the atomic number of the material (= 4) and k is a constant. Extrapolating this to 23 MeV, the fraction of the electron energy converted to photons is $P_{tot}/E = 0.004$, where we have conservatively assumed that $k = 0$. O'Dell et al. [11] have measured bremsstrahlung spectra for electron kinetic energies up to 20.9 MeV. Extrapolating these data to 23 MeV and estimating the fraction of the photon energy that exceeds the $(\gamma, 2n)$ threshold for [7]Be production, we find that about 16% of the photons are of sufficient energy to produce [7]Be. Hence, we find that the fraction of energy produced by a 23-MeV electron in thick-target bremsstrahlung that is above the threshold for [7]Be production in beryllium metal is 6×10^{-4}. To allow for inaccuracies in our estimates, we conservatively allow 10^{-3} for this value.

Lokan [5] found that the integral (γ,2n) cross section at 30 MeV is 1.2 ± 0.2 MeV-mb, and Foster and Voight [6] found that integral cross section at 45 MeV is 3.2 ± 1 MeV-mb. Extrapolating these values to 23 MeV, we estimate that the integral cross section is not more than 0.31 ± 0.05 MeV-mb.

With the estimated values of the integral cross section and the total number of ^{7}Be atoms in the limiter that might have been produced by runaways (i.e., all the activity in the unactivated tiles), an estimate can be made of the fluence of photons between 20.6 and 23 MeV that produced them. This estimate, coupled with the fraction of the energy from electrons that produced these photons, can give the electron fluence. Utilizing this electron fluence, the total number of shots and their duration can give an estimate of the average flux of 23-MeV electrons that produced the activity.

These estimates are extremely crude, based on the limited data available and the extrapolations that are made. For example, if all the ^{7}Be had been created in the early part of the experiment (e.g., the first few days) in a total period of 10 s of runaways, then it can be shown that the flux of 20.6- to 23-MeV photons constituted a power density of 2.4 kW/cm^2. This in turn implies a 23-MeV electron beam that had a power density of 2.4 MW/cm^2 over a small part of the limiter. This number is extremely hard to justify, based on the operating history of ISX-B and the hard X-ray monitor.

As another example, if the relativistic electrons had been producing ^{7}Be continuously over the life of the limiter experiment with a total exposure time of ~1000 s, then the average power density of 20.6- to 23-MeV photons would have been 40 W/cm^2 over a small part of the limiter, and this would have been produced by a relativistic electron power density of 40 kW/cm^2. This possibility is more reasonable, even though it is unlikely based on the total power measurements made on the limiter.

We cannot discount the possibility that some of the activity resulted from runaways under some fortuitous circumstance. For example, some of the high-current shots may have contained very high-energy electrons. The maximum electron energy that could be contained for 176-kA discharges is ~40 MeV. This possibility is also considered remote because of the small number of shots and the location of the runaway orbits.

Some activity can also be produced by direct electro-excitation of beryllium by direct electron impact. The cross section for this process is unknown. The early work of Guth and Mullin [12] shows that near threshold (≥ 1.67 MeV) the (γ,n) cross section exceeds the (e,e'n) cross section by about two orders of magnitude. However, this calculation does not apply to electron energies from 20 to 30 MeV and also does not apply to the (γ,2n) and (e,e'2n) processes. There is no available calculation of the (e,e'2n) cross section [which has the same threshold as the (γ,2n) process]. However, it is assumed to be small relative to the (γ,2n) cross section based on the early work.

Runaway energies of ≥ 22 MeV have been observed in the Princeton Large Torus (PLT) [13]. These measurements are based on radioactivity induced in the stainless steel limiters. In this experiment, the activity was found only within a few centimeters of the midplane on the outside of the limiter. The orbit displacement, d_γ, allowed in PLT for such particles is ~13 cm, and the maximum runaway energy allowed is calculated to be about 26 MeV for moderately peaked current profiles.

7. CONCLUSIONS AND SUMMARY

One of 12 beryllium tiles on a top limiter in the ISX-B tokamak was activated with ^{7}Be. The tokamak was operated for several months with this limiter. The spread of the radioactivity onto the other parts of the limiter and onto the vacuum vessel was studied. The activity appeared on all parts of the limiter but was particularly found on the high-field side of the originally active tile. The amount of active material found on the originally unactivated tiles is less than the mass lost from the originally activated tile. The distribution of the activity on the limiter tiles appears to indicate that $j \times B$ forces on the molten material caused a predominant movement radially inward. A small amount of active material was found in the bottom of ISX-B and probably was deposited there as molten drops of beryllium.

The isotope ^{7}Be can be generated by runaways with energies above the threshold for $(\gamma,2n)$ production. Calculations of runaway orbits show that the possibility that some of the activity observed was produced by such runaways cannot be ruled out, although it appears that the effect of runaways is probably small.

REFERENCES

[1]   P. H. Edmonds et al., "Technical Aspects of the Joint JET-ISX-B Beryllium Limiter Experiment," J. Vac. Sci. Technol., 3(3) Pt. 2 (1985) 1100–4.

[2]   P. H. Edmonds, R. D. Watson, and M. F. Smith, "Design and Fabrication of a Beryllium Limiter for ISX-B," pp. 1275–1282 in *Proceedings of the 13th Symposium on Fusion Technology, Varese, Italy, September 1984*, published as a supplement to *Fusion Technology* for the Commission of the European Communities, Pergamon Press, Elmsford, N.Y., 1984; P. H. Edmonds, P. K. Mioduszewski, J. B. Roberto, R. B. Watson, M. F. Smith, and K. J. Dietz, "The ISX-JET Beryllium Limiter Experiment," J. Nucl. Mater., **128 & 129** (1984), 422–424.

[3]   D. H. J. Goodall et al., J. Nucl. Mater., **76 & 77** (1978), 492–498.

[4]   Z. E. Switkowski et al., Radiat. Eff., **29** (1976), 65–70.

[5]   K. H. Lokan, Proc. Phys. Soc. London, **70** (1957), 836–838.

[6]   M. S. Foster and A. F. Voight, J. Inorg. Nucl. Chem., **24** (1962), 343–347.

[7]   Handbook on Nuclear Activation Cross Sections (IAEA, 1974), p. 557.

[8]   H. Knoepfel and D. A. Spong, Nucl. Fusion, **19** (1979), 785–829.

[9]   O. N. Jarvis, JET Joint Undertaking, private communication.

[10]   H. W. Koch and J. W. Motz, Rev. Mod. Phys., **31** (1959), 920.

[11]   A. A. O'Dell et al., Nucl. Instrum. Methods, **61** (1968), 340–346.

[12]   E. Guth and C. J. Mullin, Phys. Rev., **76** (1949), 234–244.

[13]   C. W. Barnes, J. M. Stavely, and J. D. Strachan, Nucl. Fusion, **21** (1981), 1469–1473.

ORNL/TM-9550
Dist. Category UC-20 f

INTERNAL DISTRIBUTION

1.	C. F. Barnett	24.	M. J. Saltmarsh
2.	J. L. Dunlap	25.	D. J. Sigmar
3–7.	P. H. Edmonds	26.	J. Sheffield
8–12.	A. C. England	27–28.	Laboratory Records Department
13.	P. K. Mioduszewski	29.	Laboratory Records, ORNL-RC
14–18.	D. L. Hillis	30.	Document Reference Section
19.	R. A. Langley	31.	Central Research Library
20.	D. A. Lee	32.	Fusion Energy Division Library
21.	J. F. Lyon	33.	Fusion Energy Division Publications Office
22.	T. Uckan		
23.	D. W. Swain	34.	ORNL Patent Office

EXTERNAL DISTRIBUTION

35. R. A. Blanken, Office of Fusion Energy, Office of Energy Research, Mail Station G-256, U.S. Department of Energy, Washington, DC 20545

36. K. Bol, Princeton Plasma Physics Laboratory, P.O. Box 451, Princeton, NJ 08544

37. R. A. E. Bolton, IREQ Hydro-Quebec Research Institute, 1800 Montee Ste.–Julie, Varennes, P.Q. JOL 2PO, Canada

38. R. L. Freeman, GA Technologies, Inc., P.O. Box 81608, San Diego, CA 92138

39. R. J. Goldston, Princeton Plasma Physics Laboratory, P.O. Box 451, Princeton, NJ 08544

40. S. W. Luke, Office of Fusion Energy, Office of Energy Research, Mail Station G-256, U.S. Department of Energy, Washington, D.C. 20545

41. E. Oktay, Office of Fusion Energy, Office of Energy Research, Mail Station G-256, U.S. Department of Energy, Washington, DC 20545

42. D. Overskei, GA Technologies, Inc., P.O. Box 81608, San Diego, CA 92138

43. W. L. Sadowski, Office of Fusion Energy, Office of Energy Research, Mail Station G-256, U.S. Department of Energy, Washington, DC 20545

44. J. W. Willis, Office of Fusion Energy, Office of Energy Research, Mail Station G-256, U.S. Department of Energy, Washington, DC 20545

45. A. P. Navarro, Division de Fusion, Junta de Energia Nuclear, Avenida Complutense 22, Madrid (3), Spain

46. Laboratory for Plasma and Fusion Studies, Department of Nuclear Engineering, Seoul National University, Shinrim-dong, Gwanak-ku, Seoul 151, Korea

47. Office of the Assistant Manager for Energy Research and Development, Department of Energy, Oak Ridge Operations, P.O. Box E, Oak Ridge, TN 37830

48. J. D. Callen, Department of Nuclear Engineering, University of Wisconsin, Madison, WI 53706

49. K. Sato, Institute of Plasma Physics, Nagoya University, Nagoya 464, Japan

Princeton Plasma Physics Laboratory, P.O. Box 451, Princeton, NJ 08544

50. H. W. Hendel
51. J. D. Strachan
52. L. R. Grisham
53. D. E. Post
54. K. M. Young
55. P H. Priester, Office of Fusion Energy, Department of Energy, Mail Stop G-256, ··· ast· igton, DC 20545
56. D. Slaughter, Lawrence Livermore National Laboratory, P.O. Box 808, Livermore, CA 94550
57. G. Gerdin, Department of Nuclear Engineering, University of Illinois, Urbana, IL 61807
58. T. P. Onak, California State University, Los Angeles, CA 90032
59. R. W. Conn, Department of Chemical, Nuclear, and Thermal Engineering, University of California, Los Angeles, CA 90024
60. S. O. Dean, Director, Fusion Energy Development, Science Applications, Inc., 2 Professional Drive, Gaithersburg, MD 20760
61. H. K. Forsen, Bechtel Group, Inc., Research Engineering, P.O. Box 3965, San Francisco, CA 94105
62. P. J. Reardon, Princeton Plasma Physics Laboratory, P.O. Box 451, Princeton, NJ 08544
63. W. M. Stacey, Jr., School of Mechanical Engineering, Georgia Institute of Technology, Atlanta, GA 30332
64. G. A. Eliseev, I. V. Kurchatov Institute of Atomic Energy, P.O. Box 3402, 123182 Moscow, U.S.S.R.
65. V. A. Glukhikh, Scientific-Research Institute of Electro-Physical Apparatus, 188631 Leningrad, U.S.S.R.
66. I. Shpigel, Institute of General Physics, U.S.S.R. Academy of Sciences, Ulitsa Vavilova 38, Moscow, U.S.S.R.
67. D. D. Ryutov, Institute of Nuclear Physics, Siberian Branch of the Academy of Sciences of the U.S.S.R., Sovetskaya St. 5, 630090 Novosibirsk, U.S.S.R.
68. V. T. Tolok, Kharkov Physical-Technical Institute, Academical St. 1, 310108 Kharkov, U.S.S.R.
69. R. Varma, Physical Research Laboratory, Navrangpura, Ahmedabad 380009, India
70. Bibliothek, Max-Planck-Institut fur Plasmaphysik, D-8046 Garching bei Munchen, Federal Republic of Germany
71. Bibliothek, Institut fur Plasmaphysik, KFA, Postfach 1913, D-5170 Julich, Federal Republic of Germany
72. Bibliotheque, Centre de Recherches en Physique des Plasmas, 21 Avenue des Bains, 1007 Lausanne, Switzerland
73. Bibliotheque, Service du Confinement des Plasmas, CEA, B.P. 6, 92 Fontenay-aux-Roses (Seine), France
74. Documentation S.I.G.N., Departement de la Physique du Plasma et de la Fusion Controlee, Centre d'Etudes Nucleaires, B.P. No. 85, Centre du Tri, 38041 Cedex, Grenoble, France
75. Library, Culham Laboratory, UKAEA, Abingdon, Oxfordshire, OX14 3DB, England
76. Library, FOM Instituut voor Plasma-Fysica, Rijnhuizen, Edisonbaan 14, 3439 MN Nieuwegein, The Netherlands
77. Library, Institute of Physics, Academia Sinica, Beijing, Peoples Republic of China
78. Library, Institute of Plasma Physics, Nagoya University, Nagoya 64, Japan
79. Library, International Centre for Theoretical Physics, Trieste, Italy
80. Library, Laboratorio Gas Ionizzati, I-00044 Frascati, Italy

81. Library, Plasma Physics Laboratory, Kyoto University, Gokasho, Uji, Kyoto, Japan
82. Plasma Research Laboratory, Australian National University, P.O. Box 4, Canberra, A.C.T. 2000, Australia
83. Thermonuclear Library, Japan Atomic Energy Research Institute, Tokai, Naka, Ibaraki, Japan
84–246. Given distribution as shown in TID-4500, Magnetic Fusion Energy (Category Distribution UC-20 f, Experimental Plasma Physics)